Simulation of Three-Dimensional Ground Motion in Los Angeles from Earthquakes in Southern California

Annual Project Summary

Award Number: 01HQGR0040
Sponsored by the U.S. Geological Survey
Dr. Kim B. Olsen, Principal Investigator
Institute for Crustal Studies
University of California at Santa Barbara
Santa Barbara, CA 93106-1100
805 893 7394
805 893 8649 (FAX)
kbolsen@crustal.ucsb.edu
Program Elements I, II
Key words: wave propagation, strong ground motion, amplification, site effects

Non-technical Summary

We have simulated wave propagation through the Southern California Earthquake Center (SCEC) velocity model 1 of the Los Angeles (LA) basin for the 1994 Northridge earthquake in order to examine the effects of anelastic attenuation and amplification in a 3D model including the sediments with shear-wave velocities (V_s) as low as 500 m/s. We find that $Q_s = 0.02\ V_s$ (m/s) in the basin sediments and much larger Q_s for deeper layers provide the best fit of synthetic and observed peak velocities for the sediments in the LA basin.

Investigations Undertaken

We use the 3D elastic model of the Los Angeles area assembled by Magistrale et al. (1998) (Figure 1) and the 1994 **M** 6.7 Northridge earthquake for our attenuation study. This earthquake is well-recorded within the basin, with relatively good signal-to-noise ratio for frequencies below 0.5 Hz. We use the combined solution from the kinematic inversion by Wald et al. (1996), with a moment of 1.3 10^{19} N m, and a one time-window, triangular slip rate function in the 3D simulations with a rise time of 1 s. The source parameters are summarized in Table 1.

The physical model is discretized with a grid spacing equivalent to 5 nodes per minimum shear wavelength of 2.5 km, the rule-of-thumb commonly used for fourth-order schemes (e.g., Levander, 1988) which limits the maximum resolved frequency to 0.5 Hz. The full model is discretized at 0.2 km grid spacing into 52.7 million grid points. Absorbing boundary conditions (Clayton and Engquist, 1977) are applied to the sides of the computational model. To further reduce artificial reflections the boundaries of the model are padded with a zone of attenuative material (Cerjan et al., 1985). The 3D modeling parameters are listed in Table 2. The scenario is kinematically simulated radially propagating outward with a constant rupture velocity of 3 km/s. The source is implemented in the finite-difference grid by adding $M_{ij}(t)/V$ to $S_{ij}(t)$ where $M_{ij}(t)$ is the $ijth$ component of the moment tensor for the earthquake, V = dx^3 is the cell volume, and $S_{ij}(t)$ is the $ijth$ component of the stress tensor on the fault at time t. The synthetic seismograms are lowpass filtered to frequencies less than 0.5 Hz (Butterworth filter with 4 poles and 2 passes). We use a staggered-grid finite-difference scheme to solve the 3D elastic equations of motion (Levander, 1988; Olsen et al., 1995; Olsen and Archuleta, 1996; Graves, 1996; Olsen et al. 2000; Olsen, 2000); the accuracy is fourth-order in space and second-order in time. The numerical implementation of the 3D scheme is described in Olsen (1994). The media parameters are averaged spatially as suggested by Moczo et al. (2001), e.g., arithmetically for densities and harmonically for Lamé parameters. We use the absorbing boundary conditions by Clayton and Engquist (1977), and the sides of the computational model are padded with homogeneous regions of attenuative material to furthermore limit reflections from the boundaries of the grid (Cerjan et al., 1985). We use the stress relaxation scheme with a coarse-grained implementation of the memory variables by Day (1998) and Bradley and Day (2000).

Results

Figure 2 shows comparisons between the log of the observed and synthetic peak velocities for data and synthetics from simulations of the Northridge earthquake using different values of Q_s, at sites within the greater Los Angeles basin. The record length of the data varies between about 30 and 60 s. However, due to poor correlation between some synthetic and recorded seismograms, we do not attempt to determine the peak velocities from the synthetics for the time interval corresponding to the data records. Instead, we assume that the true peak ground velocities were observed within the data records, and consistently compute the peak values for the synthetics from 120 s of simulated ground motion. In Figure 2b-d we explore the effect of anelastic attenuation on peak velocities for Q_s defined as fractions (0.1, 0.05, and 0.02, respectively) of V_s, compared to a loss-less

model (Figure 2a). The peak velocities of the data are overpredicted in the main LA basin for $Q_s/V_s = \infty$, 0.1 and 0.05 but are in closer agreement for Q_s/V_s=0.02. However, the fit at basin and particularly rock sites in the Santa Monica Mountains and other areas surrounding the LA basin is degraded due to excessive damping for Q_s/V_s=0.02. The underprediction at rock stations may in part be due to artificially large near-surface shear-wave velocities in the background model for the sedimentary basins.

Intuitively, Q_s/V_s may be expected to be larger than 0.02 for layers with larger V_s, which is explored in Figure 2e-g. Here, we examine the effect of using Q_s/V_s=0.1 for V_s greater than a threshold value, V_s^T). The fit for the peak velocities using V_s^T=1.5 km/s and particularly V_s^T=2 km/s are similar to that for V_s^T=∞ (Figure 2g) while V_s^T=1 km/s still generates overprediction in the NW part of the main LA basin.

Figure 2h examines the sensitivity of Q_p to the peak values. The comparison is made for V_s^T=2 km/s as in Figure 2c, but using $Q_p = Q_s(3/4)(V_p/V_s)^2$, which implies $Q(bulk) = \infty$. The fit to the peak velocities is almost identical to that for Q_p=1.5Q_s, suggesting that the peak velocities in the model are mostly insensitive to Q_p. This result is not surprising, considering an abundance of S and surface waves propagating in the LA basin for the Northridge event (Olsen, 2000).

The misfits in Figure 2 are quantified by the log standard deviation of the peak velocity residuals with an expected zero mean value in Table 3 for two sets of sites, 13 deep basin sites from the main LA basin (shown in Figure 2i) as well as for all 55 (rock and sediment) sites. The deep LA basin sediment sites are most sensitive to Q due to distances from the fault allowing surface waves to be generated, and the presence of relatively low near-surface velocities. Furthermore, they exclude rock sites where the version of the SCEC model used here may contain unrealistically large S-wave velocities outside the basin, which may cause part of the underprediction of the peak velocities observed at some rock sites. The smallest log standard deviation are obtained from the simulations using Q_s/V_s of 0.02 for V_s <1-2 km/s for both sets of sites. If only one value of Q_s/V_s is used througout the model, Q_s/V_s=0.05 provides a smaller log standard deviation compared to Q_s/V_s=0.02.

In summary, we have simulated 0-0.5 Hz 3D wave propagation in the SCEC velocity model (Version 1) of the Los Angeles basin and surrounding basins for an approximation to the **M** 6.7 1994 Northridge earthquake using various estimates of Q. The simulations show that the near-surface material with S-wave velocity of 0.5-1.0 km/s has significant effect on the ground motion, in particular above the Los Angeles basin. We find that Q_s=0.02 V_s (m/s) provides an optimal fit for the peak velocities. This is particularly the case when this relation is applied for sediments with $V_s < 1 - 2$ km/s, and much larger Q_s (0.1 V_s (m/s)) is used for higher velocities. However, Q_s for the deeper sediments is not well constrained by the simulations.

We therefore recommend the use of these estimates for Q_s in future ground motion simulations in the LA basin if sediments with V_s as low as 0.5 km/s are included. If further reduction in ${V_s}^{min}$ can be included, a refined Q_s/V_s relation may be necessary. The results are obtained using Q_p= 1.5 Q_s. However, Q_p is expectedly poorly constrained from the tests due to predominantly S and surface waves propagating in the LA basin for the Northridge earthquake.

References

Day, S.M., and C. Bradley (2001). Memory-efficient simulation of anelastic wave propagation, *Bull. Seism. Soc. Am.* **91**, 520-531.

Cerjan, C., D. Kosloff, R. Kosloff, and M. Reshef (1985). A nonreflecting boundary condition for discrete acoustic and elastic wave equations, *Geophysics* **50**, 705-708.

Clayton, R. and B. Engquist (1977). Absorbing boundary conditions for acoustic and elastic wave equations, *Bull. Seism. Soc. Am.* **67**, 1529-1540.

Day, S.M. (1998). Efficient simulation of constant Q using coarse-grained memory variables, *Bull. Seism. Soc. Am.* **88**, 1051-1062.

Graves, R.W. (1996). Simulating seismic wave propagation in 3D elastic media using staggered-grid finite differences, *Bull. Seism. Soc. Am.* **86**, 1091-1106.

Levander, A. R. (1988). Fourth-order finite-difference P-SV seismograms, *Geophysics* **53**, 1425-1436.

Magistrale, H., R. Graves, and R. Clayton (1998). A standard three-dimensional seismic velocity model for southern California: Version 1, *EOS Trans. AGU* **79**, F605.

Olsen, K.B. (1994). Simulation of three-dimensional wave propagation in the Salt Lake Basin, *Ph.D. Thesis*, University of Utah, Salt Lake City, Utah, 157 p.

Olsen, K.B., and R.J. Archuleta (1996). Three-dimensional simulation of earthquakes on the Los Angeles Fault System, *Bull. Seism. Soc. Am.* **86**, 575-596.

Olsen, K.B., R.J. Archuleta, and J.R. Matarese (1995). Three-dimensional simulation of a magnitude 7.75 earthquake on the San Andreas fault in southern California, *Science* **270**, 1628-1632.

Olsen, K.B., R. Nigbor, and T. Konno (2000). 3D viscoelastic wave propagation in the Upper Borrego Valley, California, constrained by borehole and surface data, *Bull. Seis. Soc. Am.* **90**, 134-150.

Olsen, K.B. (2000). Site amplification in the Los Angeles basin from 3D modeling of ground motion, *Bull. Seis. Soc. Am.* **90**, S77-S94.

Wald, D. J., T. H. Heaton, and K. W. Hudnut (1996). The slip history of the 1994 Northridge, California, earthquake determined from strong motion, teleseismic, GPS, and levelling data, *Bull. Seism. Soc. Am.* **86**, S49-S70.

Reports and Articles

Olsen, K.B., C. Bradley, and S.M. Day (2001). Estimation of Q and near-surface soil amplification for long-period waves in the Los Angeles basin, *Seism. Res. Lett.* **72**, 283.

Olsen, K.B., C. Bradley, and S.M. Day (2001). Estimation of Q and near-surface soil amplification for the LA basin, *Proc. SCEC Annual Meet.*, Oxnard, September 2001.

Olsen, K.B., C. Bradley, and S.M. Day (2001). Estimation of Q and near-surface amplification for long-period waves in the Los Angeles Basin, *Bull. Seis. Soc. Am.*, in preparation.

Availability of Processed Data

The simulations from which the long-period Q for the LA basin has been estimated are available from Dr. Kim Olsen, 805 893 7394, kbolsen@crustal.ucsb.edu, as peak velocities for the sites used in the study.

Table 1. Earthquake Rupture Parameters

Hypocenter Longitude, Latitude, Depth (km)	Fault Width, Length, Depth to Top (km)	Dip	Strike	Rake	Moment Magnitude
-118.53, 34.205, 17.6	22, 18, 5.0	40	122	101	6.7

Table 2. 3-D Modeling Parameters

Spatial discretization (km)	0.2
Temporal discretization (sec)	0.0125
Lowest P-wave velocity (km/sec)	0.936
Lowest S-wave velocity (km/sec)	0.5
Lowest Density (kg/m^3)	1700.
Number of timesteps	10000
Simulation time (sec)	120

Table 3. Standard Deviation of Log Peak Velocity Misfit

Q_s/V_s	Q_p/Q_s	V_s^T (km/s)	Deep Basin	All
∞	1	∞	1.14	0.82
0.01	1.5	∞	0.77	0.62
0.05	1.5	∞	0.51	0.52
0.02	1.5	∞	0.34	0.59
0.02	1.5	2	0.28	0.52
0.02	1.5	1.5	0.28	0.50
0.02	1.5	1	0.34	0.48
0.02	$(3/4)(V_p/V_s)^2$	2	0.27	0.51

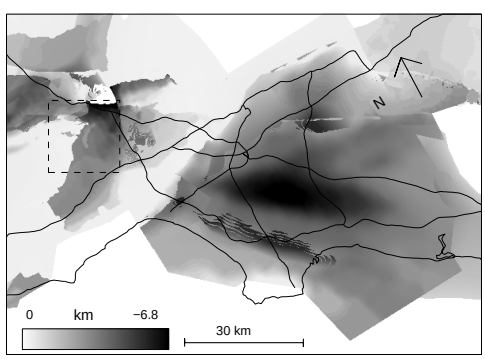

Figure 1: 3D image of the isosurface for an S-wave velocity of 2.5 km/s of the SCEC velocity model version 1. The thin solid lines depict major freeways in the modeling area and the coastline.

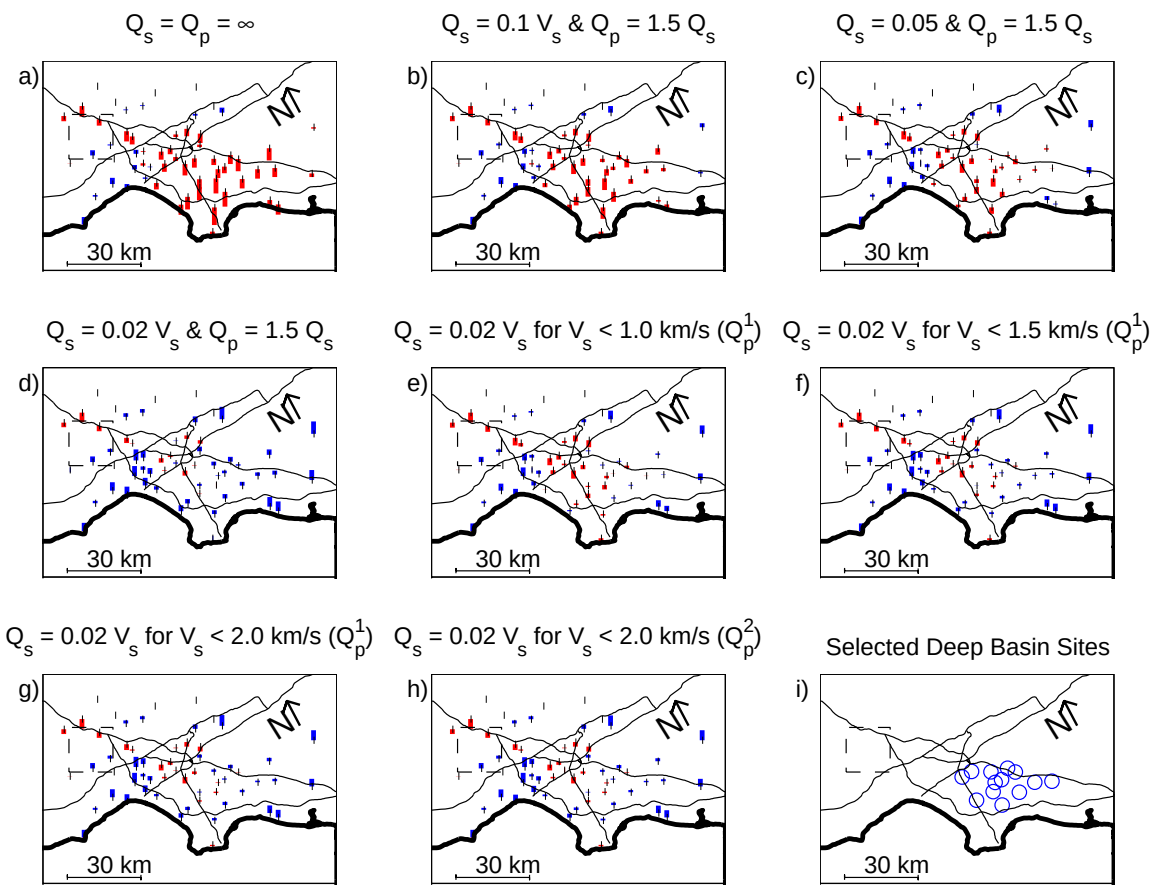

Figure 2: Difference between the log of the observed and synthetic peak velocities at 55 sites, represented by the length of the bars; blue depicts underprediction, red depicts overprediction. (a) Elastic model, (b) Q_s/V_s=0.1, (c) Q_s/V_s=0.5, and (d) Q_s/V_s=0.02. Q_s/V_s=0.02 for (e) V_s < 1.0 km/s, (f) V_s <1.5 km/s, (g) and (h) V_s <2.0 km/s. (e) - (g) use Q_p/Q_s=1.5, (h) uses $Q_p/Q_s = (3/4)(V_p/V_s)^2$. The thin solid lines depict major freeways in the modeling area and the coastline.

MODELING AND ESTIMATES OF NONLINEAR EFFECTS IN STRONG EARTHQUAKE MOTION FOR THE LOS ANGELES AREA

Award number: 01HQGR0049

Daniel Lavallée, Ralph Archuleta and Peng-Cheng Liu
Institute for Crustal Studies,
University of California, Santa Barbara,
Santa Barbara, CA 93106

Telehone numbers: 805-893-5471 (Lavallée); 805-893-8441 (Archuleta); 805-893-8231 (Liu)
Fax number: 805-893-8649
E-mail addresses: daniel@crustal.ucsb.edu; ralph@crustal.ucsb.edu; pcliu@crustal.ucsb.edu

Program Element II: Research on Earthquake Occurrence and Effects.
Key words: Wave Propagation, Strong ground motion

Non-technical summary

We have pursued the development and validation of the nonlinear model of soil dynamics using SCEC sponsored studies and strong motion data recorded during the 17 January 1994 Northridge earthquake (M_w 6.7). Measurements of ground motion observed at the Pacoima Dam Downstream (PCD or PAC) site located on bedrock, have been coupled with the nonlinear model to generate scenarios of ground shaking at the Newhall Fire Station (NWH) site. These results confirm the presence of nonlinear effects in the mainshock observed at the NWH site.